Takayama and Waragai *ROBOMECH Journal* (2023) 10:29
https://doi.org/10.1186/s40648-023-00269-5

ROBOMECH Journal

RESEARCH ARTICLE

Open Access

Coupled-driven high-speed and high-torque switchable transmission with a large transmission ratio

Toshio Takayama[1*] and Masaki Waragai[1]

Abstract

Electric motors are used globally, especially in industrial applications, and achieving high energy efficiency is a major problem. Variable transmissions are effective in reducing the energy consumption of motors, but practical variable transmissions are bulky and heavy, making them unsuitable for robots. To overcome this problem, two motor-driven mechanisms have been proposed. The two motors are operated independently and assigned to the high-speed drive and high-torque drive, and one motor always becomes dead weight. Therefore, we propose a coupled-driven switchable transmission system that can switch the high-speed and high-torque drives by combining the rotation directions and utilizing the output of both motors. The developed device uses two 22-W motors and can switch the reduction ratio from 1/15 to 1/375. The maximum torque, maximum rotation speed, and weight are 10 Nm, 500 rpm, and 905 g, respectively. The experimental results show that the relative speeds of two motors are significant for the coupled drive; nevertheless, this device can be controlled by conventional voltage control without precise speed control.

Keywords Coupled drive, Variable transmission, High-speed, High-torque

Introduction

Several types of robots are actuated by electric motors. In the last decade, the robotics market has expanded rapidly, and the number of shipments of industrial robots has doubled during the five years from 2013 to 2017 [1]. Moreover, in recent years, robots have been used not only in human-isolated environments for safety purposes, such as industrial robots, but also in areas with direct human contact, such as medical and care robots. Reducing energy consumption is currently a major challenge. While the final energy consumption in Japan has stabilized since 2005, it is increasing globally due to the development of emerging economies [2]. Considering electricity consumption, electric motors in the industrial field consume approximately 30–40% of the total electricity globally and account for approximately 70% of the total energy consumption in the industrial field [3]. Furthermore, it is certain that automobiles and other vehicles will eventually become powered by electricity. Considering these factors, increasing the efficiency of motors is an important issue.

There are two methods to increase the efficiency of motors: one is by improving the motor itself [4, 5], and the other is by improving the usage. The latter can be classified into electrical and mechanical methods, which involve control [6] and design of the transmission path of the mechanism, respectively. In terms of mechanical methods, a variable transmission gear is effective, but currently, such transmissions with practically applicable dimensions for robot joints have not been realized.

Variable transmission mechanisms can be classified into gear-switching transmissions and continuously variable transmissions (CVTs). Gear-switching transmissions use a clutch mechanism for switching gears,

*Correspondence:
Toshio Takayama
takayama.t.aa@m.titech.ac.jp
[1] Department of Mechanical Engineering, Tokyo Institute of Technology, 2-12-1 Ookayama, Meguro-ku, Tokyo 152-8552, Japan

and the reduction ratio cannot be changed while maintaining the output torque. Therefore, if a robot hand or arm is equipped with such a transmission mechanism, it will drop the object it is holding when the gear ratio is changed. By contrast, CVTs can continuously change gear ratios without losing output torque. However, practical CVTs are complicated, bulky, and not suitable for robots [7–9].

Thus, force-sensitive CVTs for robots have been studied extensively. For linear motion, linear mechanisms have been proposed [10–12]; however, they are specialized to linear motion and are not versatile. Moreover, for rotational joints, novel mechanisms have been proposed, such as a bendable linkage mechanism, twisted wire mechanism, and drum CVT mechanism, etc. [13–16]. However, these mechanisms need time to deform their transmission, cannot change the transmission ratio instantaneously; moreover, and have limited motion ranges.

Therefore, in this study, we propose a coupled-driven switchable transmission mechanism that uses two motors and can change the transmission ratio by combining the rotation directions of the two motors. The motors cooperate to drive two power transmission routes of a high-torque (low-speed) path and a high-speed (low-torque) path independently, and their rotations join again to drive the output shaft. The proposed mechanism essentially needs a non-back-drivable mechanical element so that the high torque of the high-torque path cannot back-drive the high-speed path at the joined point when the motors drive the high-torque pass. However, due to the high reduction ratio and low transmission efficiency of the non-back-drivable mechanism, it is not suitable for the high-speed path. Specifically, we have previously demonstrated that the gear ratios can be changed from 1/60 to 1/300 [17] and from 1/75 to 1/375 [18], with a small ratio of 5. Therefore, we developed a novel two-way clutch (TWC) that is a non-back-drivable mechanical element but has no reduction ratio [19]. The coupled-driven switchable transmission mechanism that uses the developed TWC can switch its reduction ratio from 1/15 to 1/375 using two 22-W motors, and the weight is only 905 g.

The remainder of this paper is organized as follows: In Sect. Methods/experimental, we show the basic principle of the coupled-driven mechanism to explain why the TWC is required. In Sect. Results, we explain the design of the proposed coupled-driven switchable transmission mechanism. In Sect. Discussion, the experimental setup and methods are explained. In Sect. Comparison with a common geared motor, the experimental results and the performance of the proposed mechanism are presented. In Sect. 6, we discuss the problems of the mechanism highlighted in the experimental results and show how to solve them. In Sect. Concluding remarks, we provide concluding remarks.

Methods/experimental

Two-way-clutch for two-motor driven high-speed and high-torque switchable mechanism

Variable transmissions can use motors at high energy efficiency, but there are presently no small variable transmission in practical use. Therefore, methods have been proposed in which two motors are independently used, one for high-speed drive and the other for high-torque drive. Their motor arrangements can be classified into two types: a parallel-arranged method [20, 21] and a serial-arranged method [22–24]. The schematics of these are shown in Fig. 1a, b, where M_1, M_2, and R indicate motor 1 for the high-speed drive, motor 2 for the high-torque drive, and a reduction gearbox for the high-torque drive, respectively. In the figure, the fixed parts are indicated with shaded lines and cannot rotate, while the parts connected to each other are indicated by a connecting link and rotate as one unit. Bearings are indicated to emphasize that they support parts rotation freely. However, for the sake of simplicity, their inclusion may be omitted when spatial constraints are a limiting factor.

In Fig. 1a, two motors are arranged in parallel. M_1 drives the output shaft directly, and thus, it has a high-speed motion with low torque. M_2 drives the output shaft via gearbox R; thus, it has a high-torque motion with low speed. However, if the shafts of M_1 and R are connected directly, M_1 cannot rotate its shaft due to the resistance of R, and as a result, this device cannot drive at high speed. Therefore, this method requires a mechanism between the output shaft and gearbox R that transmits torque only from the shaft of R to the output shaft. An electromagnetic clutch can be used for this purpose, but it makes the mechanism bulky and the control complicated. A one-way clutch or a ratchet mechanism may be employed, but such mechanisms can be driven in only one rotational direction in a high-speed drive, as shown in Fig. 2a. In this case, the mechanism shown in Fig. 2b is required so that if the input shaft is rotated the torque is transmitted to the output shaft; but if the output shaft is rotated, the shaft rotates freely and cannot transmit torque to the input shaft. Such behavior is analogous to that of a diode in electronic circuits. Thus, a torque-diode is an intuitive name for this mechanism. However, "torque-diode" is a registered trademark of NTN Corporation [25]. Therefore, in this paper, we refer to such a mechanism as a TWC (free type).

In Fig. 1b, two motors are arranged in series. M_1 is supported by a bearing, and drives the output shaft.

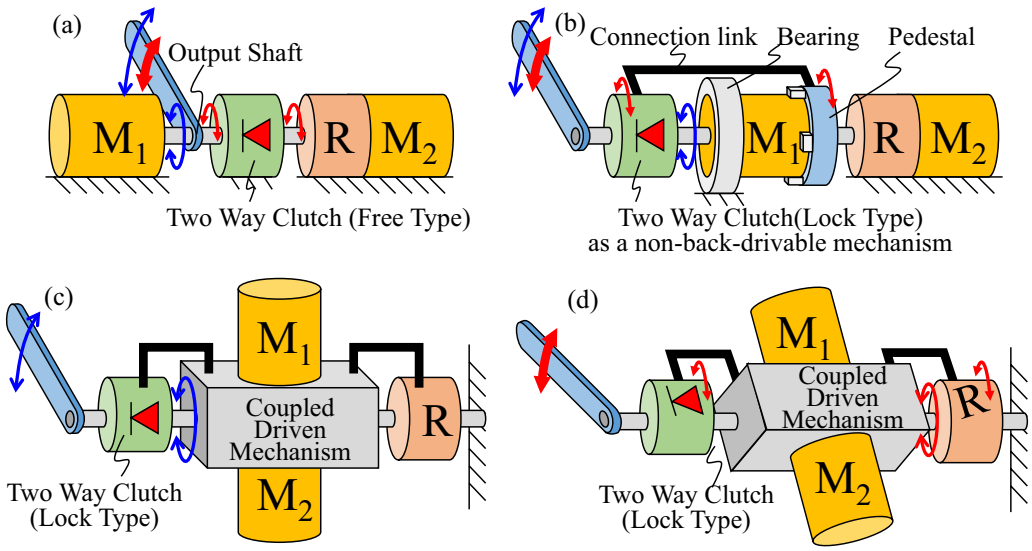

Fig. 1 Classification of two-motor driven mechanism, where **a**–**d** are parallel arrangement, serial arrangement, coupled-driven when two motors are driven in the opposite direction each other, and the coupled-driven when two motors are driven in the same direction each other, respectively

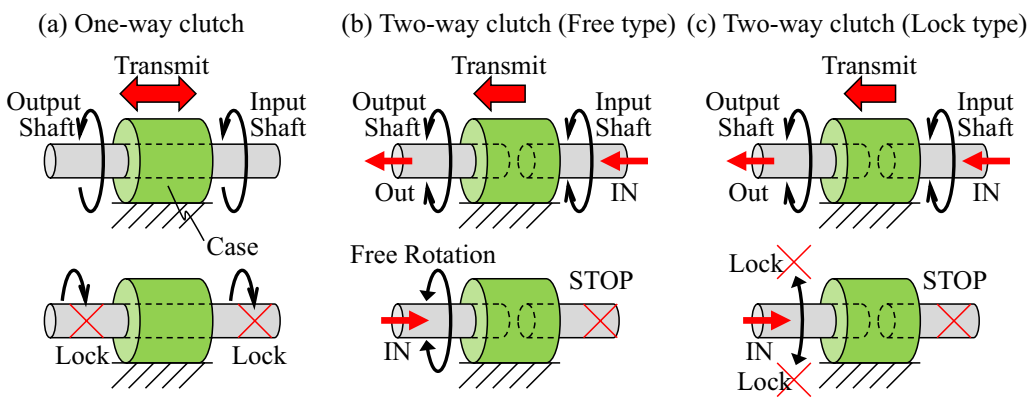

Fig. 2 The shaft rotation pattern, where **a**–**c** are one-way clutch, two-way clutch (free type), and two-way clutch (lock type), respectively

M_2 drives a pedestal via R, and the pedestal holds the entire body of M_1. If M_1 and the output shaft are connected directly, M_1 is back-driven and cannot generate a high torque when M_2 drives the entire body of M_1 by rotating the pedestal with a high torque. In this case, a non-back-drivable mechanism is needed between M_1 and the output shaft, and the pedestal is connected by a connection link. However, a conventional non-back-drivable mechanism has a high reduction ratio, screw-nut, worm gear, Shoji-Lock [26], etc., and is not suitable for high-speed driving. Therefore, the mechanical element shown in Fig. 2c is required, in which if an input torque is applied from the input shaft, the torque is transmitted to the output shaft, but if an input torque is applied from the output shaft, the shaft is locked up and cannot transmit torque to the input shaft. We call this mechanism a TWC (lock type).

As described above, the two-motor mechanism can switch high-speed and high-torque drives by using a TWC. However, these mechanisms use only one motor at high-speed or high-torque drive, and the other motor becomes a deadweight. Therefore, we proposed a coupled-driven switchable transmission mechanism, as shown in Fig. 1c, d. M_1 and M_2 are fixed to the housing of the coupled-driven mechanism, which has two output shafts on the left and right sides. When two motors are actuated in opposite directions, the left-side output shaft of the coupled-driven mechanism rotates as shown in Fig. 1c, and when two motors are actuated in the same direction, the right-side output shaft of the coupled-driven mechanism rotates as

shown in Fig. 1d. The left-side output shaft is equipped with a TWC (lock type), and the right-side output shaft is equipped with a reduction gear. Therefore, this device can switch the high-speed and the high-torque drives by using both motors' output torques. Usually, a coupled driven mechanism uses its two outputs for different works [23, 27]. However, in the proposed mechanism, two outputs are used to rotate one output; thus, they are easily interfered with each other. Therefore, it also needs a TWC (lock type). There are some TWCs that are commercially available. However, they are extremely inaccessibl and cannot rotate at high speeds because they use roller parts that generate friction inside them. Therefore, we developed a novel TWC (lock type) for this purpose [19].

Construction and design of the coupled-driven switchable transmission mechanism

Two-input & two-output coupled-driven mechanism

The actual construction of the coupled-driven mechanism is shown in Fig. 3, where D_1, D_2, G_{D1}, G_{D2}, G_{T1}, G_{S1}, G_{S2}, and R_1 are the differential gearbox 1, the differential gearbox 2, a gear fixed to the housing of D_1, a gear fixed to the housing of D_2, a gear meshed to G_{D1} and G_{D2} to rotate the input shaft of R_1, a gear attached to the output shaft of D_1, a gear attached to the output shaft of D_2, and the reduction gearbox for high-torque drive, respectively. Figure 4 shows the construction of a differential gearbox, where ω_i, ω_o, and ω_h are the rotation speeds of the input and output shafts and the housing, respectively. If the housing is fixed and the input shaft is rotated, the output shaft is rotated in the opposite direction, as shown in Fig. 4a. If the output shaft is fixed and the input shaft is rotated, the housing is rotated at half the speed of the input shaft, as shown in Fig. 4b. These relationships are expressed by the following equation:

$$\omega_h = (\omega_i + \omega_o)/2 \tag{1}$$

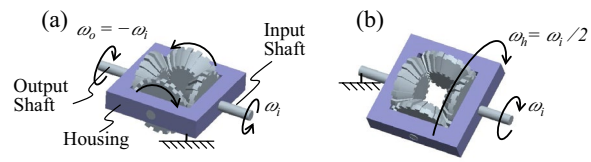

Fig. 4 The rotation pattern of a differential gearbox, where **a** and **b** are the case in which the housing is fixed and that in which the output shaft is fixed, respectively

Figure 3a shows the case where M_1 and M_2 are driven at the opposite speeds of ω and $-\omega$, respectively. In this case, D_1 and D_2 try to rotate G_{T1} by G_{D1} and G_{D2} in opposite directions but cannot rotate. As a result, G_{S1} and G_{S2} turn to rotate shaft 1 at a high speed of ω. Fig. 3b shows the case where M_1 and M_2 are driven at speeds of ω. In this case, G_{S1} and G_{S2} cannot rotate, and G_{D1} and G_{D2} rotate at a speed of $\omega/2$. As a result, G_{T1} rotates the input shaft of R_1 to rotate shaft 2 at a low speed of $\omega/2R_1$. Note that the reduction ratio R_1 includes both reduction ratios between G_{D1and2} and G_{T1} and that of R_1.

Method to combine two inputs to one output

In the example of a coupled-driven mechanism shown in Fig. 1, the motor's bodies rotate, which is not desirable because the motors are equipped with electric cables. Therefore, in the coupled-driven switchable transmission mechanism, the two outputs shown in Fig. 3 need to be combined again. In such cases, a differential gearbox is generally used. Fig. 5a shows the basic construction, where D_3 is an additional differential gearbox . A TWC is required for the high-speed drive shaft so that when the output torque is increased, the torque does not back-drive the high-speed drive shaft. This construction is robust; furthermore, as shown in Fig. 5b, we propose a

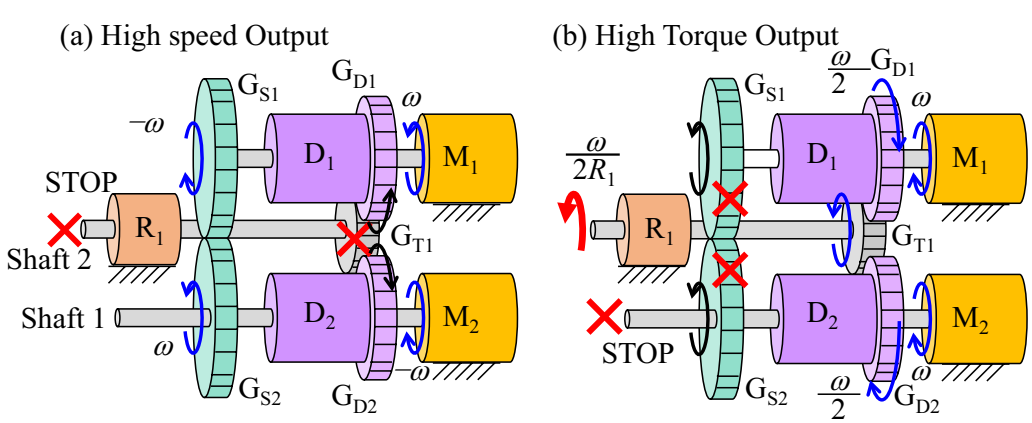

Fig. 3 Construction of the coupled driven mechanism, where **a** and **b** are high-speed output drive and high-torque output drive, respectively

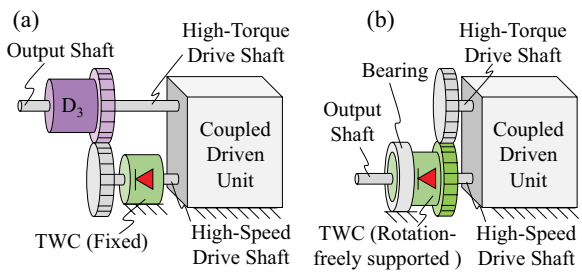

Fig. 5 Method of combining two different outputs from the coupled-driven mechanism, where **a** and **b** are the basic construction and a construction in which TWC is used as a pseudo-differential mechanism, respectively

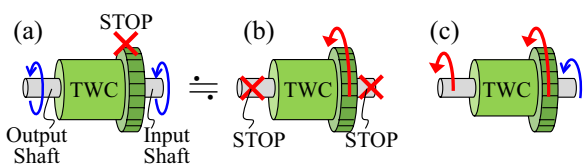

Fig. 6 The behavior of TWC to use as a pseudo-differential mechanism, where **a**–**c** are in the cases of the input shaft is rotated, the housing is rotated, both the input shaft and the housing are rotated, respectively

method in which a TWC itself is used as a pseudo-differential mechanism.

The motions of TWC used as a pseudo-differential mechanism are shown in Fig. 6. If the housing of the TWC is fixed and the input shaft is rotated, the output shaft rotates at the same speed as that shown in Fig. 6a. However, if the input shaft is fixed and the housing is rotated as shown in Fig. 6b, its relative rotation relationship between the shafts and housing is the same as that in Fig. 6a, and only the housing rotates without rotating the shafts. Therefore, to rotate the output shaft at the same speed as that of the housing, the input shaft needs to be rotated at the same speed as shown in Fig. 6c. This is the difference from an usual differential mechanism illustrated in Fig. 4. Therefore, to drive the output shaft at high torque, it is necessary to rotate the high-speed drive shaft as well as the high-torque drive shaft at the same speed. This requires a slight speed difference between M_1 and M_2 illustrated in Fig. 3b.

Total construction of the proposed mechanism

The total construction of the mechanism is shown in Fig. 7. If M_1 and M_2 rotate at the same speed in opposite directions as illustrated in Fig. 7a , the housing of the TWC is stopped and the output shaft of the TWC rotates at the same speed as that of M_1 and M_2. This motion is the high-speed drive. In this case, the reduction ratio of the high-speed drive R_{HS} is

$$R_{HS} = R_2, \tag{2}$$

where R_2 is the reduction ratio of the final gear R_2.

Moreover, if M_1 and M_2 rotate at the same speed in the same direction as shown in Fig. 3b, the TWC is driven as in Fig. 6b, and the output shaft cannot be rotated. Thus, a small difference between the speeds of M_1 and M_2 is required to rotate the input shaft of the TWC at the same rotation speed as that of the TWC housing. The motion of the high-torque drive is shown in Fig. 7b, where ω_1, ω_2, ω_{D1}, ω_{D2}, ω_{S1}, ω_{S2}, ω_{TWC}, ω_O, G_{T2}, and G_C are the rotation speeds of M_1, M_2, G_{D1}, G_{D2}, G_{S1}, G_{S2}, TWC, and the output shaft of R_2, a gear attached to the output shaft of R_1 and a gear attached to the housing of TWC, respectively. Here, the reduction ratio R_1 accounts for the total reduction ratio of the high-torque path that is enclosed with a dotted line in Fig. 7b, including the reduction ratio caused by G_{D1}, G_{D2}, G_{T1}, G_{T2}, and G_C. The relations among them are calculated as follows:

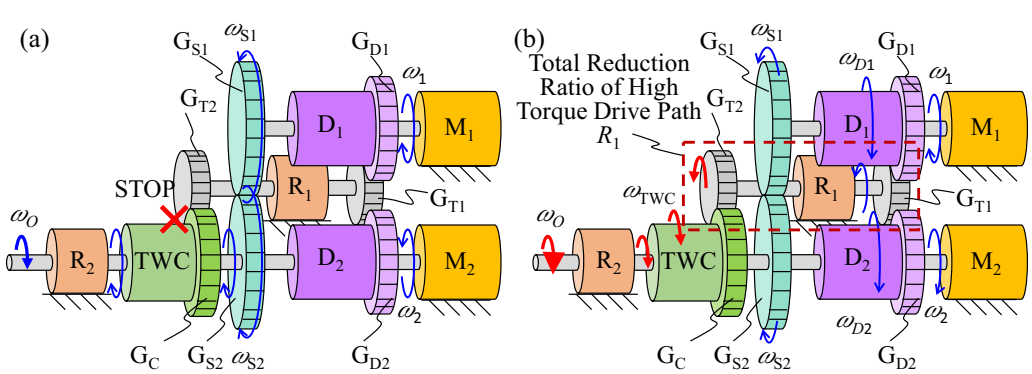

Fig. 7 Construction of the coupled driven switchable transmission mechanism, where **a** and **b** are high-speed drive motion and high-torque drive motion, respectively

$$\omega_{D1} = (\omega_1 + \omega_{S1})/2 \tag{3}$$

$$\omega_{D2} = (\omega_2 + \omega_{S2})/2 \tag{4}$$

$$-\omega_{S1} = \omega_{S2} = \omega_{TWC} \tag{5}$$

$$\omega_{D1} = \omega_{D2} = R_1\omega_{TWC} \tag{6}$$

From these equations, the speed ratio of ω_1 and ω_2 is obtained.

$$\omega_2 = \omega_1 \frac{2R_1 - 1}{2R_1 + 1} \tag{7}$$

Moreover, ω_1, ω_2, and ω_O can be calculated as follows, where R_{H1}, R_{H2}, and R_{HT} are the reduction ratios at the high-torque drive of M_1 and M_2, and the average reduction ratio at the high-torque drive, respectively.

$$\omega_1/\omega_O = R_2(2R_1 + 1) = R_{HT1} \tag{8}$$

$$\omega_2/\omega_O = R_2(2R_1 - 1) = R_{HT2} \tag{9}$$

$$R_{HT} = (R_{HT1} + R_{HT2})/2 = 2R_1R_2 \tag{10}$$

This result is equivalent to the reduction ratio obtained by the product of the reduction ratios of the differential gearboxes, R_1, and R_2. This driving method back-drives the high-speed drive path slightly and decreases the energy efficiency slightly. However, removing a differential gear can prevent the energy loss caused by the differential gear, and make the mechanism simple and small. Moreover, if R_1 is large, the back-drive speed of the high-speed path is small, and its effect is limited.

The high-torque drive can be actuated reliably by controlling the speeds of two motors using rotary encoders. In contrast, if a load torque is applied to the output of this device, the output shaft of the TWC and TWC housing are locked. Then, if the high-speed path cannot generate a high enough torque that releases the lock of TWC, it is forced to back-drive at the same speed as the rotation speed of the housing of TWC. As a result, if an appropriate load torque is applied to the output shaft, a high-torque drive can be expected without accurate speed control.

Actual design and selection of the motors and gears

The target specifications were set to an output torque of 10 Nm at the high-torque drive, a rotation speed of 500 rpm at the high-speed drive, and a switching transmission ratio of 25, referring to our previous prototype with a transmission ratio of only 5. We assumed that the maximum rotation speed of a motor was 8000 rpm. Therefore, to achieve 500 rpm at high-speed drive, the reduction ratio of R_2 is 1/16. We selected Maxon GP42C203115, whose reduction ratio, number of stages, maximum allowable torque, and weight are 1/15 (6/91), 2, 11.3 Nm, and 360 g, respectively, which approximates the desired reduction ratio. To achieve a switching transmission ratio of 25, we calculated the total reduction ratio of the high-speed path R_1= 12.5 from the following equation:

$$R_{HT}/R_{HS} = 2R_1 \tag{11}$$

If R_1 is 12.5, the actual gearbox R_1 shown in Fig. 7 is not required independently, and it can be achieved simply by the combinations of gears of D_{1and2}-G_{T1} and G_{T2}-G_C. The reduction ratio of the high-torque drive becomes $1/15 \cdot 1/25 = 1/375$.

To select motors, the transmission efficiency should be estimated. We assumed the efficiency of one gear stage as η_0. The efficiencies of a differential gearbox vary based on the motion, as shown in Fig. 4a and b. The efficiencies are

$$\eta_{Da} = \eta_0^2 \tag{12}$$

$$\eta_{Db} = \frac{1 + \eta_0^2}{2}, \tag{13}$$

where η_{Da} and η_{Db} are the efficiencies of the differential gearbox in the motion shown in Fig. 4a and b, respectively [28]. R_1 uses two sets of gear meshing, R_2 is a two-stage planetary gear, and the efficiency of the one-stage planetary gear is equal to η_{Db}. Therefore, the efficiencies of R_1 and R_2 are obtained as

$$\eta_{R1} = \eta_0^2 \tag{14}$$

$$\eta_{R2} = \left(\frac{1 + \eta_0^2}{2}\right)^2, \tag{15}$$

where η_{R1} and η_{R2} are the efficiencies of R_1 and R_2.

At the high-speed drive, the output shaft of D_1 provides torque to the input shaft of TWC via G_{S1} and G_{S2}, but the output shaft of D_2 provides torque to the input shaft of the TWC directly. Thus, we assumed the efficiency of G_{S1} and G_{S1} as their average η_{GS}

$$\eta_{GS} = \frac{1 + \eta_0}{2} \tag{16}$$

From these, the efficiencies of the high-speed drive η_{HS} and high-torque drive η_{HT} can be calculated as follows:

$$\eta_{HS} = \eta_{Da}\eta_{GS}\eta_{R2} = \eta_0^2\left(\frac{1 + \eta_0^2}{2}\right)^2\left(\frac{1 + \eta_0}{2}\right) \tag{17}$$

$$\eta_{HT} = \eta_{Db}\eta_{R1}\eta_{R2} = \eta_0^2\left(\frac{1+\eta_0^2}{2}\right)^3 \tag{18}$$

By assuming $\eta_0 = 0.9$, we can assume $\eta_{HS} = 0.63$ and $\eta_{HT} = 0.60$.

To achieve maximum torque at the high-torque drive $T_{HTmax} = 10$ Nm, the rated torque of the motor T_N should satisfy the following equation:

$$T_N > \frac{T_{HTmax}}{2\eta R_{HT}} = 22[\text{mNm}] \tag{19}$$

To achieve maximum speed at the high-speed drive $n_{HSmax} = 500$ rpm, the rated rotation speed of the motor n_N should satisfy the following equation:

$$n_N > R_{HS}n_{HSmax} = 7500[\text{rpm}] \tag{20}$$

Based on the above criteria, we selected Maxon DC-MAX26GBKL24V with a rotary encoder, whose nominal voltage, nominal torque, nominal speed, nominal current and weight are 24 V, 26.6 Nm, 8100 rpm, 1.08 A, 120 g, respectively.

Figure 8 shows the actual arrangement of the mechanical elements of the coupled-driven switchable transmission mechanism. The actual photo is shown in Fig. 9. The specifications are also shown in the figure. Details of all gears and their stiffness are shown in Appendix A

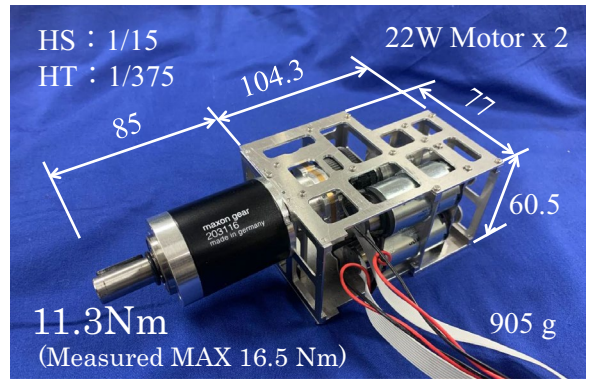

Fig. 9 Developed coupled-driven high-speed and high-torque switchable transmission with its specifications

Experimental method

The motors are driven by Maxon's motor drivers (ESCON module 24/2). The motor driver can drive a motor in two ways: one is voltage control, where the driver outputs a voltage equivalent to a specified rotation speed based on pre-measured data without using the rotary encoder. The other is precise speed control using the rotary encoder. Owing to its versatility, experiments were primarily conducted using voltage control and partially using speed control. For safety, the current limit was set to 1.08 A, which is the maximum continuous current, and the acceleration limit is set to 30000 rpm/s. The following experiments were conducted.

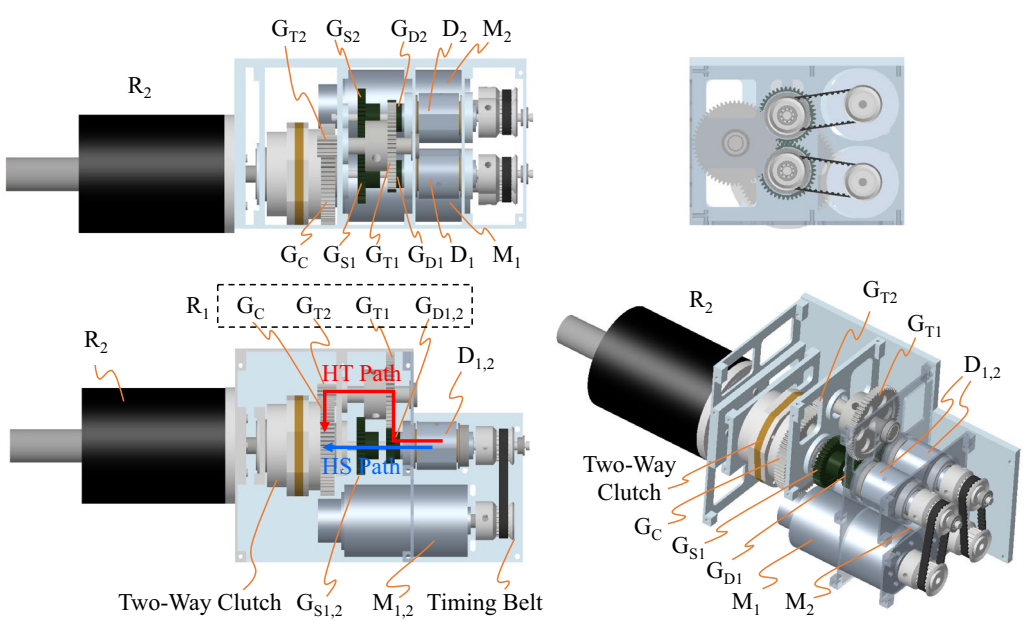

Fig. 8 Three-directinal view and perspective bird's-eye view of the 3D-CAD model

Experiment to confirm the switching of the high-speed drive and the high-torque drive

Exp. 1-1 High-speed drive by the voltage control In the high-speed drive, two motors are driven at the same speed. The motor drivers supply a voltage equivalent to 4000 rpm to the two motors. After 5 s of forward rotation, 5 s of inverse rotation is conducted.

Exp. 1-2 The high-torque drive by the speed control In the high-torque drive, a speed difference is required between the two motors. First, we confirmed that the device can be driven using the high-torque drive by accurately controlling the motor speed. M_1 is driven at 4000 rpm and M_2 is driven at 12/13 of that speed. This ratio is obtained from eq. 7.

Exp. 1-3 The high-torque drive by the voltage control In a simple device such as an in-vehicle winch directly connected to the battery via a relay switch without using a motor driver, the speed difference between the two motors should be generated naturally without complicated control. In the developed device, if two motors are driven at the same speed, the housing of TWC will rotate freely. However, when a load is applied to the output, the TWC may lock, which could potentially generate a speed difference between the two motors naturally. We attached an arm of 180-mm length to the output shaft and attached a weight of 0.6 kg that applies a torque of approximately 1.1 Nm to the shaft, as shown in Fig. 10. Then, we moved the arm upward for 5 s, then downward. The experiment was conducted using different voltages at equivalent to 1000 rpm and 4000 rpm.

Exp. 1-4 Torque switching experiment We conducted a torque-switching experiment assuming that the robot hand grasps an object, where the finger switches the drive modes from the high-speed drive to the high-torque drive after the finger touches the object. An arm of 170-mm length is attached to the output shaft and pushed against a force sensor (Tec Gihan, USL06-H5-200N-A) to measure the contacting force, as shown in Fig. 11. The screw of the slitted part is tightened so that the arm does not slip against the output shaft. The applied voltage is changed from that used at equivalent to 1000 rpm to that at 4000 rpm. Moreover, we confirmed the maximum output torque of this device when the nominal current of 1.08 A is applied to the motors at the high-torque drive.

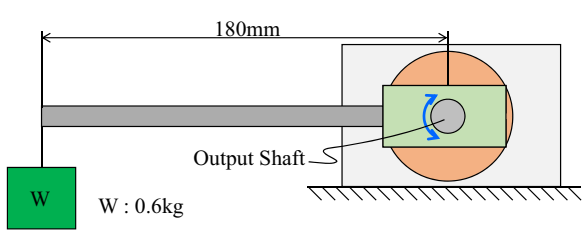

Fig. 10 Experimental setup for the high-torque drive by the voltage control

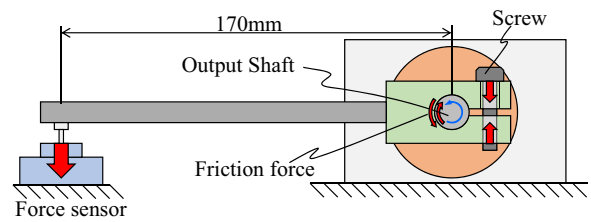

Fig. 11 Experimental setup for the torque measurement experiments

Experiment to measure the transmission efficiency

Exp. 2-1 Static torque transmission efficiency The experimental setup is the same as that in Exps. 1–4 (Fig. 11), and we changed the supplying voltages and calculated the input torque of the motors from their currents. The static torque efficiency η_S, can be calculated by the following equation, where T_{out}, T_{in1}, T_{in2}, T_{in}, and R are the output torque of the device, torque of M_1, that of M_2, total torque, and reduction ratio of the device, respectively. R denotes R_{HS} for the high-speed drive and R_{HT} for the high-torque drive.

$$\eta_S = \frac{|T_{out}|}{(|T_{in1}| + |T_{in2}|)R} = \frac{1}{R}\frac{|T_{out}|}{|T_{in}|} \tag{21}$$

Exp. 2-2 Dynamic power transmission efficiency The experimental setup to measure the dynamic power transmission efficiency is the same as that for Exp. 1–4 (Fig. 11). The screw of the slitted part is tightened softly such that the output shaft can make a slip. When the output shaft is rotated, the torque is transmitted by the friction between the output shaft and slitted parts. Since the transmitted torque cannot be set arbitrarily, we change the tightening torque of the screw to collect experimental data. In this experiment, two motors are driven by speed control so that the speed of M_1 approximates 1000 rpm and 4000 rpm.

The input power P_{in}, output power P_{out}, and dynamic power efficiency η_D can be calculated by the following equation, where n_{M1}, n_{M2}, and n_{out} are the rotation speed of M_1, M_2, and the output shaft, respectively.

$$\eta_D = \frac{P_{out}}{P_{in}} = \frac{|T_{out}n_{out}|}{|T_{M1}n_{M1} + T_{M2}n_{M2}|} \tag{22}$$

In the case of the high-speed drive, two motors are driven at the same speed but in opposite directions, thus $n_{M1} = -n_{M2}$, and the relation of the motor speed and output shaft speed becomes $|n_{M1}| = |R_2 n_{out}|$. Thus, the

dynamic power efficiency in the high-speed drive η_{DHS} can be calculated by the following equation.

$$\eta_{DHS} = \frac{T_{out}}{(T_{M1} - T_{M2})R_2} = \frac{1}{R_{HS}} \frac{T_{out}}{T_{in}} \tag{23}$$

In the case of the high-torque drive, we need to consider that the two motors are driven at different speeds and their reduction ratios are different.

$$\eta_{DHT} = \frac{T_{out}}{T_{M1}R_{HT1} + T_{M2}R_{HT2}} = \frac{T_{out}/R_{HT}}{T_{M1}R_{HT1}/R_{HT} + T_{M2}R_{HT2}/R_{HT}} = \frac{1}{R_{HT}} \frac{T_{out}}{T'_{in}} \tag{24}$$

where T'_{in} is the equivalent input torque including the difference in reduction ratios of the two motors. In the experimental results, we show plots of these values.

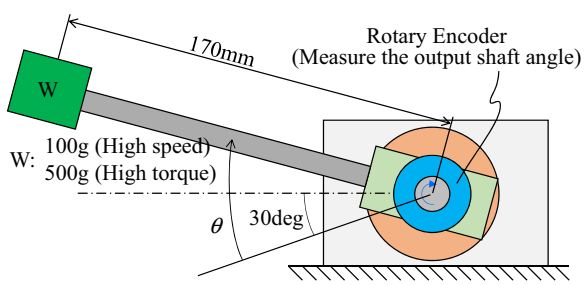

Fig. 12 Experimental setup for feed back control

Experiment to confirm the applicability of feedback control

If the device is used in applications such as a robot arm, feedback control is needed, and the use of TWC may cause problems in feedback control due to its backlash. Thus, we conducted basic feedback experiments. Fig. 12 shows the experimental setup. The arm lifts a weight from θ values of 0° to 60° where $\theta = 0$ is 30° lower than the horizontal line. Weights of 100 g and 500 g were used for the high-speed drive and the high-torque drive, respectively. The rotation angle of the output shaft was used for the feedback value, and motors were controlled by the voltage control. In the high-torque drive, the applied voltage of the slower motor is 12/13 of that of the faster motor. We conducted P control (Exp. 3-1) and PID control (Exp. 3-2) experiments.

Results

Results of experiment 1

Res. 1-1 Experimental results of the high-speed drive by the voltage control The experimental result is shown in Fig. 13a We confirmed that M_1 and M_2 rotate at approximately 4000 rpm and the output shaft rotates at approximately 250 rpm, and its reduction ratio is 1/16. The actual reduction ratio is slightly smaller than the ideal reduction ratio of 1/15. We assumed that this is due to a small difference in the characteristics of two motors, where the high-torque drive path is slightly moving. Moreover, after this experiment, we applied a rated voltage of 24 V to both motors and confirmed that both motors rotate at approximately 7950 rpm. Therefore, the rotational speed

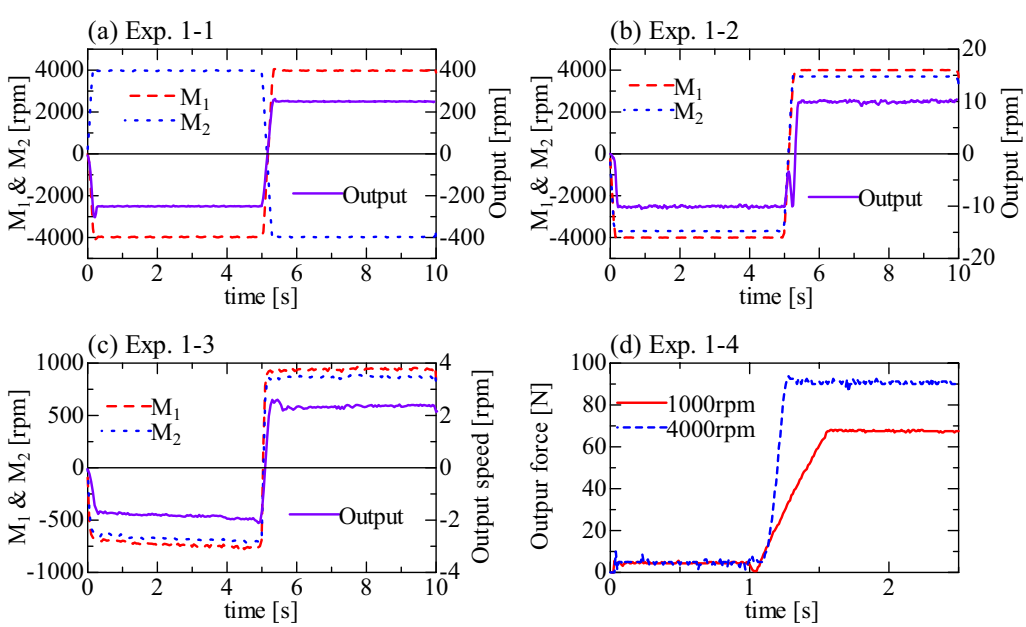

Fig. 13 Experimental result of the high-speed drive and the high-torque drive, where **a**–**c** are results of exp. 1-1, 1-2, 1-3, and 1-4, respectively

of the output shaft was slightly smaller than 500 rpmapproximately close as designed.

Res. 1-2 Experimental result of the high-torque drive by the speed control The experimental result is shown in Fig. 13b. When motors are controlled by rotary encoders, the high-torque drive is driven as expected.

Res. 1-3 Experimental result of high-torque drive by the voltage control When the motors are driven at the same voltage as that at equivalent to 1000 rpm, the two motors were synchronized and the speed difference between them was generated naturally. Thus, the high-torque drive worked as expected, as shown in Fig. 13c. Moreover, when the motors were driven at the same voltage as that at equivalent to 4000 rpm, the output shaft could not be driven and the housing of TWC rotated similar to that in the condition shown in Fig. 5b. This phenomenon can be prevented following the condition discussed in Sect. 4.

Res. 1-4 Experimental result of torque switching The experimental results are shown in Fig. 13d. In both experiments where the applied voltages are equivalent to those at 1000 rpm and 4000 rpm, the output torques could be switched. When the applied voltage was small, the output force was momentarily reduced due to the backlash of the TWC, which is not desirable. However, when the applied voltage was large, such a force reduction did not appear, and it could change the reduction ratio faster compared to when the applied voltage was small. Moreover, when we applied a nominal current of 1.08 A to the motors, the measured torque was 16.5 Nm. It exceeded the maximum allowable torque of the gear box, and the target specification of 10 Nm was achieved.

Results of experiment 2

Res. 2-1 Experimental result of static torque transmission efficiency The measured input torques and output torques are shown in Fig. 14. A first-order approximation of the experimental values is shown by the solid line in the figure. Since the output torque should be 0 when the input torque is 0, the graph was approximated such that it intersects the origin, as shown by the dashed line. Although both lines are close, the x-intercept of the solid line is slightly positive and the slope of the solid line is slightly larger than that of the dashed line. This means that the efficiency increases with increasing input torque. We assumed that this was caused by a constant friction force that is not affected by the applied input torque. Since the transmission efficiency is the slope of the dashed line divided by the gear ratio, the average efficiencies of the high-speed drive and high-torque drive are 0.69 and 0.89, respectively. In this experiment there are no dynamic losses, thus, both efficiencies are larger than the theoretical values of η_{HS}=0.63 and η_{HT}=0.6.

Res. 2-2 Experimental result of the dynamic power transmission efficiency Experimental results of the relationship between the input torque and the output torque are shown in Fig. 15a, b. The x-intercepts of all graphs are far from the origin, and thus, we calculated the efficiencies as shown in Fig. 15c, d. When the input torque becomes small, the efficiency decreases significantly. In the range of the graph, the efficiencies do not converge to their maximum values. The estimation of the maximum efficiency will be discussed in Sect. Discussion.

Experimental results of feedback control

Res. 3-1 Experimental result of P control First, we conducted P control experiments. Experiments were conducted using different P gains *Kp* of 2 and 4. The values were selected experimentally. Figure. 16 shows the experimental results. In the high-speed drive, the experimental result shows an overshoot when $Kp = 4$. It shows discontinuous motions due to the backlash of the TWC. By contrast, in the high-torque drive, overshoot did not occur even when we used larger *Kp* than this experiment, and discontinuous motions could not be generated. Moreover, in both experiments, a position deviation remained.

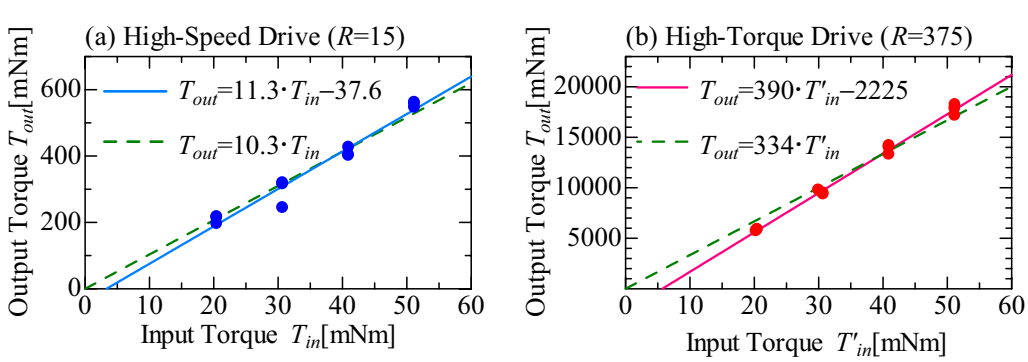

Fig. 14 Experimental result of the static torque transmission efficiency, where **a** and **b** are output torque by the high-speed drive, and output torque by the high-torque drive, respectively

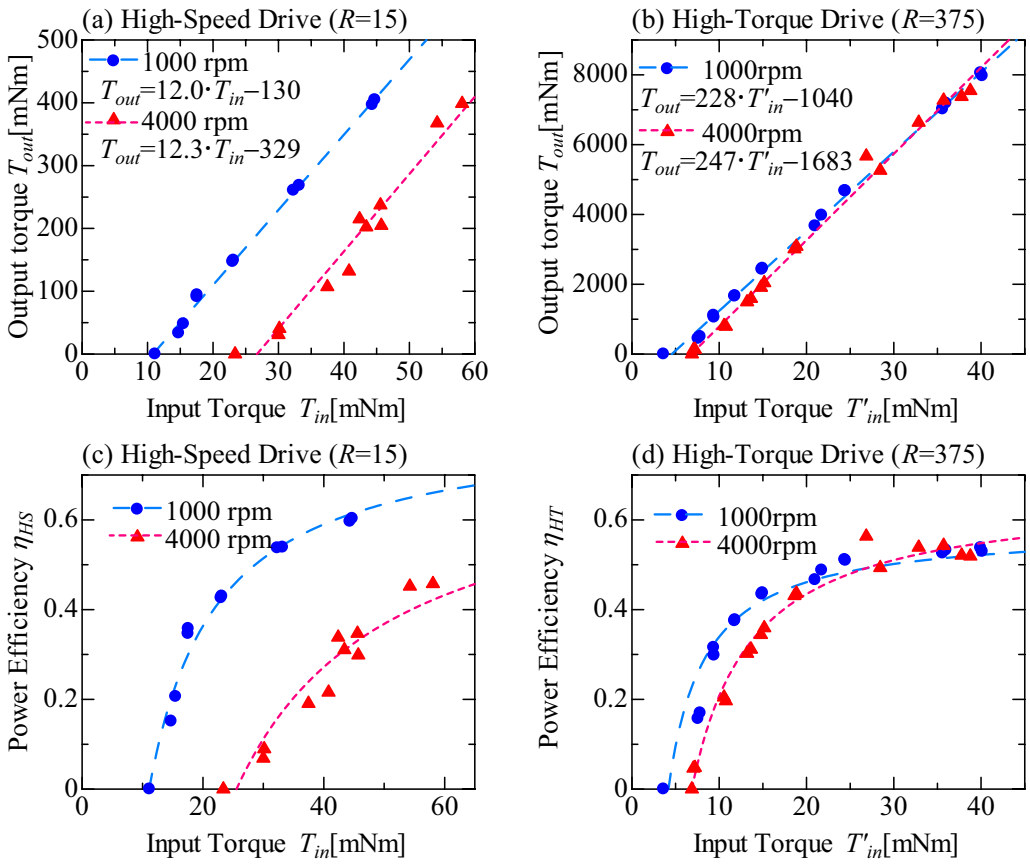

Fig. 15 Experimental result of the dynamic power transmission efficiency, where **a**–**d** are output torque by the high-speed drive, power efficiency by the high-speed drive, output torque by the high-torque drive, and power efficiency by the high-torque drive, respectively

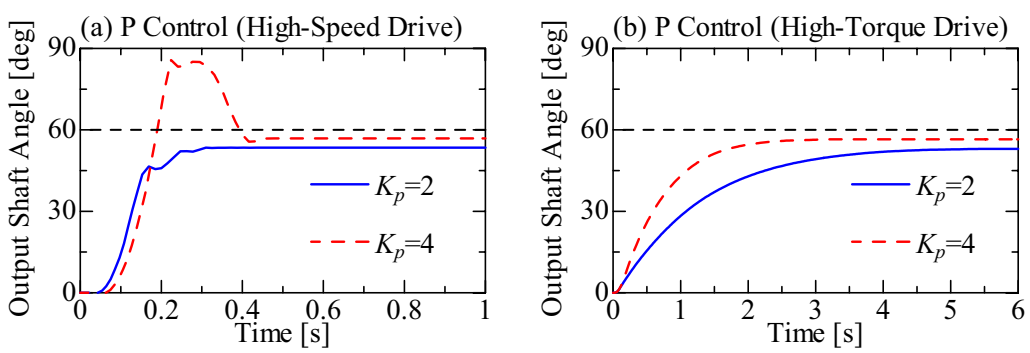

Fig. 16 Experimental result of P control where **a** and **b** are experiment by the high-speed drive, and by the high-torque drive, respectively

Res. 3-2 Experimental result of PID control To remove position deviations, we experimented with PID control. Since the backlash effect did not occur in the high-torque drive, we conducted a PID control experiment only for the high-speed drive. The gains were experimentally obtained by trial and error. The experimental result is shown in Fig. 17. The output approached to the target angle, but a discontinuous vibration remained because of the backlash of the TWC. The reduction of this vibration will be discussed in Sect. Discussion.

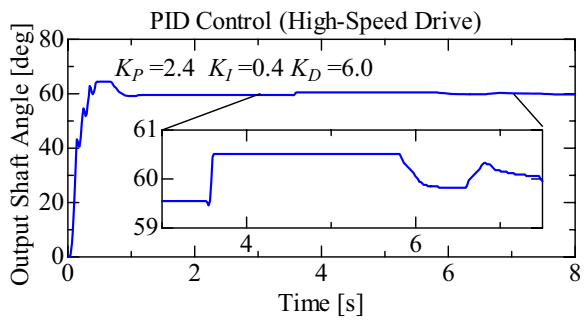

Fig. 17 Experimental result of PID control

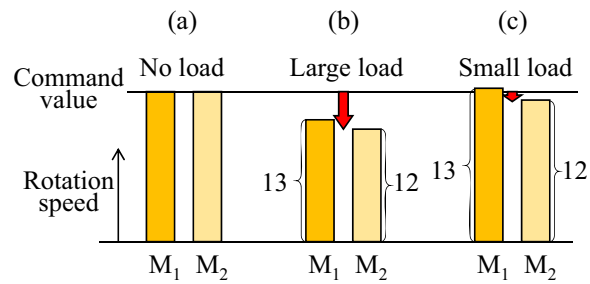

Fig. 19 Images of the actual speed reduction where **a**–**c** are conditions of no load, large load, and small load, respectively

Discussion

High-torque drive by the voltage control

The proposed device worked almost exactly as expected. However, when the two motors were driven at the same voltage without speed control at the high-torque drive, they naturally synchronized and could be driven when the applied voltage was equivalent to that at 1000 rpm. However, the motors could not be driven when the applied voltage was equivalent to that at 4000 rpm. We assumed that the applied load to the output shaft was small compared to the input torques. Thus, we additionally experimented with the same voltage equivalent to 3000 rpm applied to the motors, and confirmed that the two motors were naturally synchronized to drive the high-torque drive. The experimental result is shown in Fig. 18a. The motor currents are also shown. In this experiment, the current of M_1 becomes negative, which means M_2 forces to rotate M_1 to generate counterelectromotive force, which is an undesirable situation for using two motors effectively.

This phenomenon can be considered, as shown in Fig. 19. The command values of the voltages for the two motors are the same. If the load of the output shaft is zero, the housing of the TWC rotates freely because the two motors rotate at the same speed as that shown in Fig. 19a. If the load is applied to the output shaft sufficiently, the motors are forced to synchronize at the speed ratio of 13:12. If the applied load is high, as shown in Fig. 19b, both actual rotation speeds are slower than the commanded value and both motors work. However, if the load is small, the rotation speed of M_1 exceeds the commanded value, as shown in Fig. 19c, resulting in the current of M_1 flowing backward. To avoid this phenomenon,

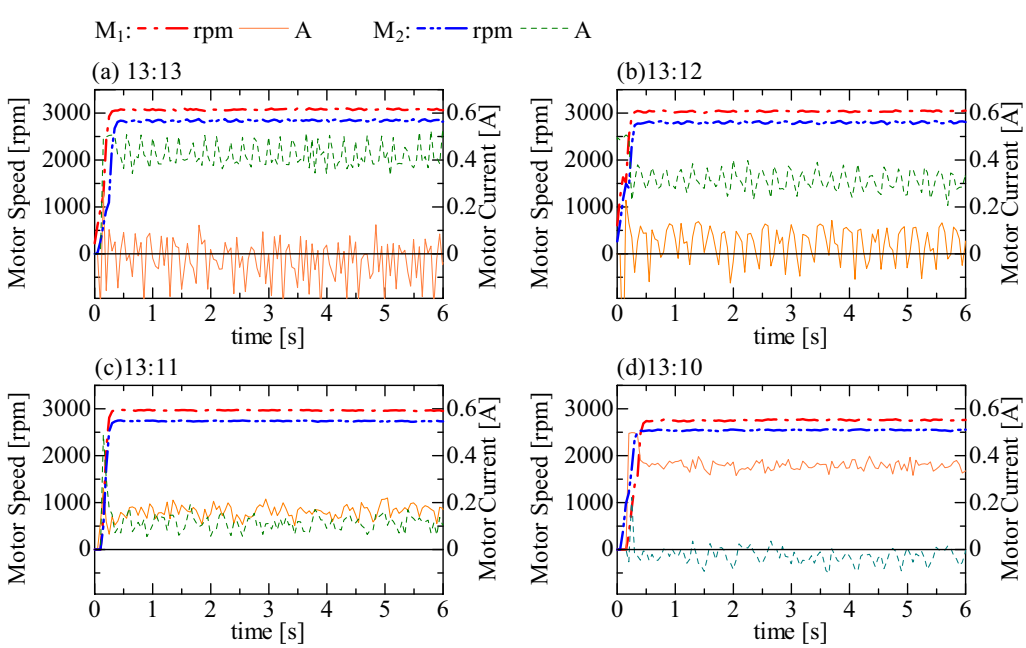

Fig. 18 Experimental result of the voltage control of the high-torque drive

the commanding value should be different. Ideally, the speed ratio of the two motors is 13:12, and in the PID control experiment, the device works correctly by applying the voltages at a ratio of 13:12. Therefore, we conducted additional experiments where the voltages ratios were changed to 13:12, 13:11 and 13:10, as shown in Fig. 18b–d. When the ratio of the voltages was 13:12, the current of M_1 became positive, but remained lower than that of M_2. When the ratio was 13:11 the currents of both motors were approximately equal. When the ratio was 13:10, the current of M_2 became negative. These results show that it is not always advisable to apply the voltages to the motors based on theoretical ratios. Whether this phenomenon is due to machining accuracy or the principle of this mechanism needs to be investigated in the future.

If the load torque is not sufficient, automatic synchronization of two motors by applying the same voltage cannot be realized, but synchronization is seen if voltages with the adequate ratio are applied. Although this device is not suitable for use in direct connection with a battery, the experimental result shows that it has a possibility of switching the high-speed drive and high-torque drive only by controlling the voltage, such as through an inverter, without complicated speed control system.

Assumption of the maximum dynamic power transmission efficiency

The dynamic torque transmission efficiency differs significantly depending on the input torque because it can be assumed that there are two types of losses: one is a loss μ_c that depends only on the rotation speed and the other is a loss μ_r that depends not only on the rotation speed but also on the input torque. By using these, the following equation is obtained.

$$T_{out} = (1 - \mu_r)T'_{in}R_{HT} - \mu_c, (1 > \mu_r > 0, \mu_c > 0) \tag{25}$$

The approximation curves in Fig. 15c, d are obtained using this equation, and the parameters are shown in Table 1. Based on this equation, the efficiency converges to $1 - \mu_r$ if the input torque is unlimited, and its values at the high-speed drive and high-torque drive are approximately 0.8~0.82 and 0.6~0.65, respectively. The estimated value of the high-speed drive becomes larger than the theoretical value, and that of the high-torque drive becomes close to the theoretical value. In practice, there is an upper limit to the input torque, so the efficiency of the high-speed drive is expected to reach approximately 0.72, which is the static torque transmission efficiency.

Table 1 Assumed parameters for the power transmission efficiency

Drive mode	rpm	μ_r	μ_c
High-speed	1000	0.202	8.65
	4000	0.179	21.94
High-torque	1000	0.392	2.77
	4000	0.340	4.49

Modified PID control for this mechanism

When the device is controlled by PID in the high-speed drive, vibrations remain due to the backlash of TWC. Therefore, we introduced a control method where the integrated value of current control is reset to 0 when the deviation P is less than 0.3 degrees, that is, 10 pulses in the encoder, and the rotation speed D is 0. The experimental result is shown in Fig. 17. It can stop stably and the deviation error becomes smaller than 0.03 deg. This result shows that PID control is available even in the high-speed drive that has a backlash by allowing a small deviation (Fig. 20).

Comparison with a common geared motor

The developed device uses two 22-W DC motors, can switch two reduction ratios at a different ratio of 25, and can achieve a maximum output torque of 10 Nm and maximum rotation speed of 500 rpm. We consider the case where this value is achieved by a geared motor without a variable transmission. The maximum motor rotation speed does not differ significantly due to its wattage. To withstand the same output torque, the gear head used is the same as that for our final gear with a reduction ratio and weight of 1/15 and 360 g, respectively. Assuming that the efficiency of the gear head is 85%, to achieve an output torque of 10 Nm, the required motor torque is higher than 784 mNm. This value is 14.7 times larger compared to the summed value of 53.2 mNm of the two motors used in the developed device (26.6 mNm×2). Thus, the wattage of the desired motor is 22 W×2 × 14.7 = 647 W.

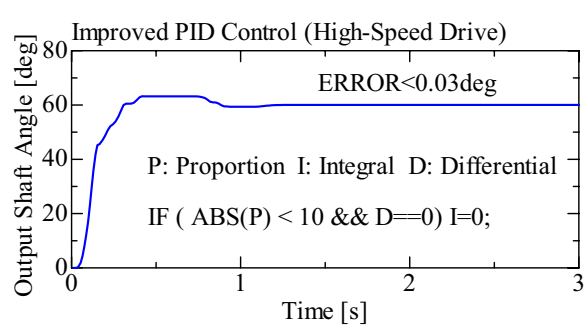

Fig. 20 Experimental result when improved PID control is applied to the high-speed drive

Table 2 Specifications of the used gear

Palameters		Coupled Drive					TWC		$D_{1,2}$
	Symbol	$G_{S1,2}$	$G_{D1,2}$	G_{T1}	G_{T2}	G_C	Planetary gear	Internal gear	Bevel gear
Module	m	0.5							
Pressure angle	α	20							
Number of teeth	Z	40	24	60	14	70	23	60	
Facewidth	b [mm]	3	3	3	5	5	3	3	2.5
Outer cone distance	R_a [mm]								7.1
Rotational speed (Initial assumption)	n [rpm]	7500	3750	1500	1500	300	0	0	7500
Maximum load	T [mNm]	36.5	40.6	183	183	823	78.8	205	40.6
Call circumference force	F_t [N]	3.65	6.77	6.77	52.3	52.3	13.7	13.7	1.37
Material		POM	POM	S45C	S45C	S45C	S45C	C3604	C3604
Allowable material stress at the root	σ_{lim} [N/mm]	39.2	39.2	137	137	137	137	26.2	26.2
Tooth form factor	Y_F			2.28	3.2	2.25	2.68	2.07	2.93
Load distribution factor	Y_ϵ			0.591	0.625	0.625	0.508	0.508	0.61
Helix angle factor	Y_β			1	1	1	1	1	1
Life factor	K_L			1	1	1	1	1	1
Dimension factor	K_{FX}			1	1	1	1	1	1
Dynamic load factor	K_V			1.5	1.5	1.5	1.2	1.2	1.7
Overload factor	K_O			1	1	1	1	1	1
Tooth form factor	y	0.7	0.415						
Speed correction factor	K_v	1.12	1.36						
Temperature factor	K_T	1	1						
Lubrication factor	K_l	0.75	0.75						
Material factor	K_M	0.75	1						
Service factor	C_S	0.8	0.8	Assumed 3 hrs/day					
Safety factor	S_F	1.2							
Cutter diameter effect factor	Y_C								1
Longitudinal load distribution factor	K_D								1.8
Reliability factor	K_R								1.4
Allowable circumference force	F_{tlim} [N]	27	26	85	95	135	112	28	3.0

If the weight and size of the motor is proportional to its wattage, the weight of the required motor becomes 120 g$\times 2 \times 14.7 = 3528$ g, and the total weight including the gear head becomes 3888 g. As a result, this device succeeded in reducing the size and weight significantly. Moreover, at the high-torque drive, the developed device has a high reduction ratio with a low current, and thus, the energy consumption can also be reduced. It should be noted, of course, that this device cannot produce both high-speed and high-torque at the same time.

Concluding remarks

In this paper, we showed that a two motor-driven high-speed and high-torque switching mechanism essentially requires a TWC to achieve a high variable transmission ratio. Additionally, we proposed a coupled driven switchable transmission mechanism that uses a novel TWC to achieve a high variable reduction ratio. Experimental results show the proposed device works as expected. Moreover, its usability and controllability are also discussed. However, the experiments in this paper were conducted independently for high-speed and high-torque drive, respectively, and how to switch the gear ratio during position control is an interesting topic for

taking advantage of the characteristics of the device. In the future, we will conduct such experiments. Moreover, we will develop a different type of TWC (free type) to develop a parallel arranged motor type two motor-driven mechanism as another method of two motor-driven mechanisms.

Appendix A Specifications of the used gears

The stiffness of the gears can be calculated based on the gear technical referencebook [29]. We selected all gears for the allowable circumference force F_{tlim} to exceed the call circumference force F_t as listed in Table 2

F_{tlim} of a metal-spur gear can be obtained by the following equation.

$$F_{tlim} = \sigma_{lim} \frac{mb}{Y_F Y_\epsilon Y_\beta} \frac{K_L K_{FX}}{K_V K_O} \frac{1}{S_F}, \tag{A1}$$

where σ_{lim}, m, b, Y_F, Y_ϵ, Y_β, K_L, K_{FX}, K_V, K_O and S_F are module, facewidth, tooth form factor, load distribution factor, helix angle factor, life factor, dimension factor, dynamic load factor, overload factor and safety factor, respectively.

F_{tlim} of a plastic-spur gear can be obtained by the following equation.

$$F_{tlim} = myb\sigma_{lim} \frac{K_v K_T K_l K_M}{C_S} \frac{1}{S_F}, \tag{A2}$$

where y, K_v, K_T, K_l, K_M and C_S are tooth form factor, speed correction factor, temperature factor, lubrication factor, material factor and service factor, respectively.

F_{tlim} of a bevel gear used inside differential gear box $D_{1,2}$ can be obtained by the following equation.

$$F_{tlim} = 0.85\sigma_{lim} \frac{R_a - 0.5b}{R_a} \frac{mb}{Y_F Y_\epsilon Y_\beta Y_C} \frac{K_L K_{FX}}{K_D K_V K_O} \frac{1}{K_R}, \tag{A3}$$

where R_a, Y_C, K_D and K_R are, outer cone distance, cutter diameter effect factor, longitudinal load distribution factor and reliability factor, respectively.

Acknowledgements
Not applicable.

Author contributions
TT proposed the device, analyzed the experimental data, and wrote the draft. MW assembled the device, conducted the experiments, and analyzed the data. Both authors read and approved the final manuscript.

Funding
This work was supported by JKA and its promotion funds from KEIRIN RACE.

Availability of data and materials
The datasets used and/or analysed during the current study are available from the corresponding author on reasonable request.

Declarations

Competing interests
The authors declare that they have no competing interests

Received: 2 October 2023 Accepted: 4 December 2023
Published online: 19 December 2023

References

1. on Robotics for Social Change C Environmental Changes Surrounding Robots and Future Policy Directions -Plan to promote social transformation through robotics- (in Japanese) (2019). https://www.meti.go.jp/shingikai/mono_info_service/robot_shakaihenkaku/pdf/20190724_report_01.pdf Accessed 10 Sep 2023
2. White Paper on Energy (in Japanese) (2022) https://www.enecho.meti.go.jp/about/whitepaper/2022/pdf/whitepaper2022_all.pdf Accessed 10 Sep 2023
3. Ito M, Morinaga S (1999) High-efficiency motor (in Japanese). J Japan Soc Appl Electromagn Mech 7(3):45–48
4. Tokoi H, Kawamata S (2012) Study of high-efficiency motors using soft magnetic core (in Japanese). IEEJ Trans Ind Appl 132–D(5):574–580
5. Kosaka T, Ozeki A, Matsui N (2016) Drive characteristics of high efficiency hybrid excitation motor for automobiles (in Japanese). J Japan Soc Appl Electromagn Mech 24(3):246–251
6. Tong Y, Morimoto J, Morimoto S, Takeda Y, Hirasa T (1992) High efficiency control of brushless dc motors for energy saving (in Japanese). Trans IEE Japan 112–D(3):285–291
7. NSK Co L Toroidal CVT Powertoros Unit. https://www.nsk.com/jp/products/automotive/drive/hcvt/ Accessed 10 Sep 2023
8. Honda Co L Hydraulic mechanical CVT. https://www.honda.co.jp/DN-01/equip/transmission/ Accessed 10 Sep 2023
9. Takako Industries I Compact HST. https://www.takako-inc.com/products/pdf/hst.pdf Accessed 10 Sep 2023
10. Hirose S, Hagiwara T (1999) Development of x-scmw: a load-sensitive actuator incorporating a variable transmissions. Proceedings 1999 IEEE International Conference on Robotics and Automation, 193–199
11. Takaki T, Yamasaki Y, Ishii I (2011) Load-sensitive continuously variable transmission using an oblique feed screw for parallel-jaw grippers. Proceedings 2011 International Symposium on Micro-NanoMechatronics and Human Science, 507–510
12. Tadakuma K, Tadakuma R, Terada MA, Kazuki and Shimojo M, Higashimori M, Kaneko M (2011) The mechanism of the linear load-sensitive continuously variable transmission with the spherical driving unit. Proceedings 2011 IEEE/RSJ International Conference on Intelligent Robots and Systems, 4048–4053
13. Takaki T, Omata T (2006) 100g-100n finger joint with load-sensitive continuously variable transmission. Proceedings 2006 IEEE International Conference on Robotics and Automation, 976–981
14. Godler I, Kohtaroh HJ, Sonoda T (2010) Robotic finger with coupled joints: a prototype and its inverse kinematics. Proceedings 2010 11th IEEE International Workshop on Advanced Motion Control (AMC) 28(6):337–342
15. Shin YJ, Lee HJ, Kim K-S, Kim S (2012) A robot finger design using a dual-mode twisting mechanism to achieve high-speed motion and large grasping force. IEEE Trans Rob 28(6):1398–1405
16. Matsushita K, Shikanai S, Yokoi H (2009) Development of drum cvt for a wire-driven robot hand. Proceedings 2009 IEEE/RSJ International Conference on Intelligent Robots and Systems, 2251–2256
17. Takayama T, Arakawa T, Omata T (2012) Coupled driven variable transmission unit (in Japanese). Trans Japan Soc Mech Eng 78(794):3541–3551
18. Takayama T, Kudo H, Omata T (2016) Output torque transition of the coupled driven variable transmission mechanism (in Japanese). Proceedings 2016 JSME Conference on Robotics And Mechatronics, 2–1052
19. Waragai M, Takayama T (2022) Development of a high-speed and low-torque loss two-way clutch. ROBOMECH J 10
20. Ohnaga H, Takenawa S (2012) A study on high speed / large grasping force driving joint using one-way clutch (in Japanese). Proceedings 2012 JSME Conference on Robotics And Mechatronics, 1–204

21. Kimura H, Tamura T, Katano K, Shimizu T, Akira I (2009) Development of power transmission change system with paradox gear reduction (in Japanese). Proceedings 2009 JSME Annual Conference, 27–28
22. Takaki T, Omata T (2009) High-performance anthropomorphic robot hand with grasping-force-magnification mechanism. IEEE/ASME Trans Mechatron 16(3):583–591
23. Bao Y, Takaki T (2022) Manipulator equipped with differential wrist mechanism to combine the torque of two motors to increase fingertip force and wrist torque. IEEE Robot Automation Lett 7(4):10025–10032
24. Takayama T, Yamana T, Omata T (2012) Three-fingered eight-dof hand that exerts 100-n grasping force with force-magnification drive. IEEE/ASME Trans Mechatron 17(2):218–227
25. Office JP Trademark registration No. 4566654. https://www.j-platpat.inpit.go.jp/t0302 Accessed 10 Sep 2023
26. Katsuharu S About the new self-lock mechanism. https://www.shoji-lock.jp/pdf/shoji-lock.pdf Accessed 10 Sep 2023
27. Hirose S, Nishihara T (1995) Development of powerful manipulator raiden-1. basic design used fdm and fdm-cd. (in Japanese). Proceedings The 13th RSJ Annual Conference, 731–732
28. Morozumi M (1975) On the efficiency formulas of differential gears (in Japanese). J Faculty Eng 38:45–55
29. Kohara Gear Industry Co L Gear Technical Reference. https://khkgears.net/new/gear_knowledge/gear_technical_reference/ Accessed 16 Nov 2023

Publisher's Note